The midregion, nuclear localization sequence, and C terminus of PTHrP regulate skeletal development, hematopoiesis, and survival in mice

Ramiro E. Toribio,*,[1] Holly A. Brown,* Chad M. Novince,[§] Brandlyn Marlow,* Krista Hernon,* Lisa G. Lanigan,[†] Blake E. Hildreth III,[†] Jillian L. Werbeck,[†] Sherry T. Shu,[†] Gwendolen Lorch,[†] Michelle Carlton,[‡] John Foley,[¶] Prosper Boyaka,[†] Laurie K. McCauley,[§,‖] and Thomas J. Rosol[†]

*Department of Veterinary Clinical Sciences and [†]Department of Veterinary Biosciences, College of Veterinary Medicine, and [‡]Wright Center of Innovation in Biomedical Imaging, The Ohio State University, Columbus, Ohio, USA; [§]Department of Periodontics and Oral Medicine and [‖]Department of Pathology, Medical School, University of Michigan, Ann Arbor, Michigan, USA; and [¶]Medical Sciences Program, Indiana University School of Medicine, Bloomington, Indiana, USA

ABSTRACT **The functions of parathyroid hormone-related protein (PTHrP) on morphogenesis, cell proliferation, apoptosis, and calcium homeostasis have been attributed to its N terminus. Evidence suggests that many of these effects are not mediated by the N terminus but by the midregion, a nuclear localization sequence (NLS), and C terminus of the protein. A knock-in mouse lacking the midregion, NLS, and C terminus of PTHrP (*Pthrp*$^{\Delta/\Delta}$) was developed. *Pthrp*$^{\Delta/\Delta}$ mice had craniofacial dysplasia, chondrodysplasia, and kyphosis, with most mice dying by d 5 of age. In bone, there were fewer chondrocytes and osteoblasts per area, bone mass was decreased, and the marrow was less cellular, with erythroid hypoplasia. Cellular proliferation was impaired, and apoptosis was increased. *Runx2*, *Ocn*, *Sox9*, *Crtl1*, β-*catenin*, *Runx1*, *ephrin B2*, *cyclin D1*, and *Gata1* were underexpressed while *P16/Ink4a*, *P21*, *GSK-3*β, *Il-6*, *Ffg3*, and *Ihh* were overexpressed. Mammary gland development was aberrant, and energy metabolism was deregulated. These results establish that the midregion, NLS, and C terminus of PTHrP are crucial for the commitment of osteogenic and hematopoietic precursors to their lineages, and for survival, and many of the effects of PTHrP on development are not mediated by its N terminus. The down-regulation of *Runx1*, *Runx2*, and *Sox9* indicates that PTHrP is a modulator of transcriptional activation during stem cell commitment. Toribio, R. E., Brown, H. A., Novince, C. M., Marlow, B. Hernon, K., Lanigan, L. G., Hildreth III, B. E., Werbeck, J. L., Shu, S. T., Lorch, G., Carlton, M., Foley, J., Boyaka, P., McCauley, L. K., Rosol, T. J. The midregion, nuclear localization sequence, and C terminus of PTHrP regulate skeletal development, hematopoiesis, and survival in mice. *FASEB J.* 24, 1947–1957 (2010). www.fasebj.org**

Key Words: parathyroid · osteoblast · craniofacial · lethality

Parathyroid hormone-related protein (PTHrP), first described as the humoral mediator of cancer-associated hypercalcemia (1–3), is a pleiotropic factor with multiple physiological functions, including regulation of morphogenesis, cell proliferation and differentiation, and transplacental calcium transport (4). The biological functions of PTHrP have been attributed to its N terminus [PTHrP-(1–34)], which binds to the parathyroid hormone (PTH) receptor 1 (PTH1R) (2, 5). While PTH is an endocrine factor exclusively produced by the parathyroid glands to regulate calcium and phosphorus homeostasis, PTHrP functions as an autocrine, paracrine, and intracrine factor in fetal and adult tissues (6). Mice with ablation of the *Pthrp* gene (*Pthrp*$^{-/-}$) are characterized by chondrodysplasia, accelerated chondrocyte differentiation and endochondral ossification, and lethality within minutes of birth, demonstrating that PTHrP is critical for survival and skeletal morphogenesis (7, 8). PTHrP is also essential in integument biology; the lack of PTHrP or the PTH1R results in failure of mammary gland development (9–11).

Although the emphasis of most research has been on PTHrP interacting with the PTH receptor, the ontogenic relevance of other domains is intriguing. There is evidence that many of the effects of PTHrP on cell proliferation, apoptosis, and transepithelial calcium transport are mediated by the midregion, a nuclear localization sequence (NLS), and the C terminus. The midregion of PTHrP increases transplacental calcium transport (12, 13), and PTHrP-(67–86) and PTHrP-(38–94) are the most active midregion fragments (12, 13). Cell culture studies indicate that PTHrP has a NLS that inhibits apoptosis and promotes cell proliferation (14, 15). PTHrP-(67–94) interacts with importin β and GTP-Ran to promote its translocation into the nucleus (16, 17). A nuclear targeting sequence that inhibits

[1] Correspondence: Department of Veterinary Clinical Sciences, The Ohio State University, 601 Vernon Tharp St., Columbus, OH 43210, USA. E-mail: toribio.1@osu.edu

doi: 10.1096/fj.09-147033

apoptosis exists at PTHrP-(87–107) (15, 18–20), and PTHrP-(109–139) is involved in its nuclear export (21). PTHrP also has been implicated in pancreatic β-cell function, where it increases insulin production (22). Amino, midregion, and C-terminal fragments of PTHrP have been measured in humans under physiological and pathological conditions (23–25); however, their roles are poorly understood. These findings suggest that PTHrP must be produced in proximity to its target cells; thus, it is primarily autocrine and paracrine in nature. The significance of the putative NLS and C terminus was recently demonstrated in mice expressing PTHrP-(1–84), which showed growth retardation and lethality (26).

In this study, we evaluated the *in vivo* relevance of the midregion, NLS, and C terminus of PTHrP by generating knock-in mice expressing PTHrP-(1–66), thus lacking these domains, but preserving the N-terminal functions of PTHrP. Knock-in mice had abnormal skeletal development, impaired hematopoiesis, aberrant mammary gland development, dysregulated energy metabolism, and early lethality, confirming the hypothesis that many of the effects of PTHrP on development are not mediated by its N terminus. Moreover, our study also provides evidence that the midregion of PTHrP participates in development because compared to mice expressing PTHrP-(1–84) (26), mice expressing PTHrP-(1–66) have a more severe phenotype.

MATERIALS AND METHODS

Generation of *Pthrp*$^{\Delta/\Delta}$ mice

This study was approved by The Ohio State University Institutional Animal Care and Use Committee. To generate the *Pthrp*$^{\Delta/\Delta}$ mice, exon 4 was replaced by an exon 4 lacking the sequence encoding for PTHrP-(67–137). RNA splicing was predicted with GenScan (http://genes.mit.edu/GENSCAN.html). Deletion was carried out *via* PCR with Tgo polymerase (Roche, Indianapolis, IN, USA) to leave blunt ends (see Supplemental Data). The targeted 1.1-kb exon 4 was flanked by a 5.5-kb intronic long arm at the 5′ end, and a 1.1-kb intronic short arm at the 3′ end (Supplemental Fig. S1*A*). A *Spe*I restriction site was introduced between exon 4 and the long arm to facilitate Southern blotting. Fragments were cloned into *pPNT* to generate the final construct (*pPNT-PTHrP*$^{\Delta/\Delta}$). The construct was linearized with *Not*I, and 10 μg of DNA was electroporated into SV129/SvEv ES cells. Clones were selected with G418, screened for homologous recombination by PCR, confirmed by Southern blot analysis, and injected into E4.0 C57BL/6 blastocysts. Male chimeras were bred to C57BL/6 females, and offsprings were selected on the basis of agouti coat color, PCR, and Southern blot analysis. Mice with homologous recombination were bred to C57BL/6 *EIIa-Cre* mice to excise the *Neo*^{r} cassette and generate the breeding line (*Pthrp*$^{+/\Delta}$).

For Southern blot analysis, genomic DNA was digested with *Spe*I, fractionated in a 0.5% agarose gel, transferred onto nylon membranes, and hybridized with a 700-bp DNA probe. This resulted in an 8.4-kb fragment in wild type and 7.0- and 8.4-kb fragments in recombinants. For the 3′ end, DNA was digested with *Bam*HI and screened with a 1-kb DNA probe, resulting in 7.5 kb for wild-type and 7.5 and 9.5 kb (+*Neo*^{r} cassette) fragments for recombinants (Supplemental Fig. S1*A*). Sex was determined by PCR of the *Sry* gene. Primers used in this study are listed in Supplemental Table S1.

Microcomputed tomography (micro-CT) and bone morphometry

Whole pups and skull and long bone specimens were evaluated with a high-resolution micro-CT system (Siemens, Nashville, TN, USA). Images were reconstructed with IRW (Siemens) and analyzed with bone morphometry software (Ratoc System Engineering, Tokyo, Japan). Settings used were as follows: pups = 20 × 40, 400 projections, bin of 2, exposure = 575 ms, energy = 80 kV, current = 500 mA, and 34.7-μm isotropic voxel size; head = 33 × 9, 400 projections, bin of 1, exposure = 340 ms, energy = 80 kV, current = 500 mA, and 12.00-μm voxel size; bone specimens = 12 × 17, 380 projections, bin of 1, exposure = 2175 ms, energy = 70 kV, current = 100 mA, and 10.00-μm isotropic voxel size. Variables analyzed included bone volume/total volume (BV/TV), bone surface area/bone volume (BS/BV), trabecular thickness (Tb.Th), trabecular number (Tb.N), trabecular spacing (Tb.Sp), cortical wall thickness (C.Th), and bone mineral density (BMD). See Supplemental Data.

Skeletal double-staining

Pups were euthanized, eviscerated, skinned, and fixed in 95% ethanol for 48 h. Placement in acetone for 48 h allowed residual fat removal. Skeletons were double-stained at room temperature with 0.015% w/v Alcian blue and 0.005% w/v Alizarin red S in a 1:9 mixture of acetic acid and 70% ethanol for 48 h. After staining, pups were washed twice with distilled water and immersed in 1% KOH for 48 h to remove additional soft tissue. Skeletons were cleared in increasing concentrations of glycerol (from 20 to 100%) over a 2-wk period.

Hematology, blood chemistry, hormones, and bone markers

Total calcium concentrations were measured with a colorimetric assay (BioAssay Systems, Hayward, CA, USA). Serum triglycerides, phosphorus, glucose concentrations, and alkaline phosphatase activity were analyzed with a biochemistry analyzer (Roche Hitachi, Indianapolis, IN, USA). Hemograms were performed manually in a veterinary hematology laboratory. Mouse-specific enzyme immunoassays were used to determine the serum concentrations of PTH (Alpco, Salem, NH, USA), osteocalcin (Biomedical Technologies, Stoughton, MA, USA), TRAP 5b (IDS, Scottsdale, AZ, USA), and insulin (Alpco). Plasma PTHrP concentrations were determined with a 2-site immunoradiometric assay (DSL, Webster, TX, USA).

Histology and histomorphometry

Tissue specimens for histological evaluation were fixed in 10% buffered formalin at 4°C for 24 h, embedded in paraffin, cut in 4-μm sections, and stained with hematoxylin and eosin (H&E). In addition, bone specimens were decalcified in 10% EDTA (pH 7.4) at 4°C for 1–7 d. Fetal bone specimens were not decalcified. For skin examination, embryonic day (E)18.5 fetuses and neonate skin were fixed in 10% cold buffered formalin for 24 h, and subsequently in cold 70% ethanol. Mammary tissue was assessed by serial sectioning. Images were acquired with an automated microscopy system (Aperio Technologies, Vista, CA, USA) and quantification performed with ImagePro Plus (Media Cybernetics, Bethesda, MD, USA). For

TRAP staining, the leukocyte acid phosphatase kit (Sigma-Aldrich, St. Louis, MO, USA) was used.

Immunohistochemistry and TUNEL staining

For PTHrP, a goat polyclonal anti-human PTHrP-(1–34) (Santa Cruz Biotechnology, Santa Cruz, CA, USA) was used at 1:100 dilution, and the secondary antibody was biotinylated rabbit anti-goat IgG (Vector Laboratories, Burlingame, CA, USA) at 1:200 dilution. For caspase-3, a rabbit polyclonal anti-mouse antibody (Cell Signaling, Danvers, MA, USA) was used at 1:200 dilution. For Ki-67, a rat monoclonal anti-mouse antibody (Dako, Carpinteria, CA, USA) was used at 1:100 dilution. For von Willebrand factor, a rabbit polyclonal anti-mouse antibody (Dako) was used at 1:1000 dilution. To assess apoptosis *via* TUNEL, we used the Apoptag Plus Peroxidase Kit (Millipore, Billerica, MA, USA) and the *In Situ* Cell Death Detection Kit, POD (Roche).

Proliferation of primary chondrocytes and osteoblasts

Growth plates from newborn pups were harvested, rinsed with PBS, minced, and digested at 37°C for 2 h with 1 mg/ml of collagenase A (Roche) and 0.25% trypsin/EDTA (Invitrogen, Carlsbad, CA, USA) in α-minimum essential medium (α-MEM) without FBS, at 60 rpm. Tissue was mixed by gently pipetting 10 times. After 2 h, the remaining tissue was allowed to sediment, and less-dense tissue was harvested. The cell suspension was filtered through a 70-μm cell strainer (BD Biosciences, San Jose, CA, USA), rinsed with PBS, counted, and plated at a density of 100,000 cells/well in α-MEM, 10% FBS, penicillin (100 U/ml), and streptomycin (100 μg/ml). Chondrocyte proliferation was assessed by plating 15,000 cells/well in 24-well plates. Cells were counted in triplicate at 24, 48, and 72 h. For osteoblasts, calvariae were dissected from 2-d-old mice, isolated from periosteum, and subjected to sequential digestions of 10, 20, and 30 min with 2 mg/ml of collagenase A and 0.25% trypsin. Cells from the third digestion were harvested. Proliferation and viability was assessed with the MTT assay (Promega, Madison, WI, USA). PTHrP-(1–141) was generated in LCC15-MB transfected cells with the human PTHrP-(1–141) cDNA; PTHrP-(1–86) was commercially available (Abcam, Cambridge, MA, USA); and PTHrP-(67–139) was chemically synthesized (GenScript, Piscataway, NJ, USA).

Von Kossa staining

To assess *in vitro* mineralization, primary calvarial osteoblasts were plated in 12-well plates at 13,500 cells/cm^2. On reaching confluency, cultures were treated with mineralization medium (α-MEM, 10% FBS, penicillin, streptomycin, 50 μg/ml ascorbic acid and 10 mM β-glycerophosphate) for 21 d. Cultures were performed in triplicate, and medium was changed every other day. At the end of the culture period, cells were fixed with 95% EtOH and stained with 5% $AgNO_3$ using the von Kossa method.

Osteoclastogenesis

Spleens were dissected from 2-d-old mice, and dissociated using a 70-μm cell strainer (BD Biosciences) and the plunger of a 1-ml syringe. Mononuclear cells were isolated *via* Ficoll (Sigma-Aldrich) gradient centrifugation. Cells were plated on glass slides coated with apatite-collagen complexes in 24-well plates at 9.5×10^4 cells/cm^2. Cells were cultured in α-MEM, 10% FBS, penicillin, and streptomycin. Osteoclastogenesis was induced with 30 ng/ml of RANKL (R&D Systems, Minneapolis, MN, USA) and 50 ng/ml of M-CSF (R&D Systems). Medium was changed every other day. On d 6, cells were fixed in citrate-buffered acetone/formaldehyde for 1 min and stained for TRAP activity (Sigma-Aldrich). Red-stained TRAP$^+$ multinucleated (≥3 nuclei/cell) cells were enumerated, and results were expressed as number of osteoclasts per well.

Flow cytometry

Primary chondrocytes were cultured for 48 h and treated with camptothecin (10 μM) for 4 h. After treatment, cells were rinsed with cold PBS, detached with 0.05% trypsin, centrifuged 5 min at 200 *g* in PBS, resuspended in annexin V binding buffer, treated with FITC annexin V and propidium iodide (Invitrogen) for 15 min, and submitted to flow cytometry in a FACSCalibur system (BD Biosciences). The cell population in the bone marrow and spleen was assessed using the CD3 (PE), CD11b (FITC), CD11c (APC-Cy7), and B220 (PerCP-Cy5.5) cell markers. Cells were collected in RPMI with 5% FBS, segregated with a syringe plunger, washed in RPMI, centrifuged at 200 $g \times 5$ min, and resuspended in FACS buffer (PBS+1% BSA+0.01% sodium azide) to a density of 1×10^6/ml (100 μl). Primary antibody (20 μl) was added for 30 min at 4°C, cells were centrifuged in 500 μl of FACS buffer, resuspended in 100 μl of FACS buffer with 20 μl of secondary antibody, and submitted to flow cytometry (1×10^4 cells were counted). Lin$^-$Sca-1$^+$c-Kit$^+$ cell population was assessed in the bone marrow. Antibodies were purchased from BD Biosciences (San Diego).

Quantitative real-time PCR

Total RNA was extracted with TRIzol reagent (Invitrogen) and submitted to a second extraction step using RNA isolation columns and DNase I (Stratagene, La Jolla, CA, USA). Complementary DNA (cDNA) was synthesized using Superscript reverse transcriptase (Invitrogen) or the First Strand Kit (SABiosciences, Frederick, MD, USA). Initial gene expression profiling was carried out with mouse-specific osteogenic, stem cell, and apoptosis PCR arrays (SABiosciences). Real-time PCR was performed under standard methods, using SYBR Green mix and a Lightcycler 480 (Roche). Gene expression was normalized by the GeNorm geometric averaging (27) of multiple mouse housekeeping genes (*B2m, Hprt1, Ubc, Gapdh, Ppia*). Cycling conditions were 94°C, 15 min, followed by 40 cycles of 94°C, 15 s; 57°C, 20 s; 72°C, 10 s. Primers are listed in Supplemental Table S1.

Western blot analysis

Tissue was pulverized in liquid nitrogen and homogenized in ice-cold lysis buffer (100 mM NaCl, 50 mM Tris HCl, 1 mM EDTA, 1mM Na_3VO_4, 1 mM NaF, 1 mM PMSF, 10% Triton X-100, and 5 μg/ml each of leupeptin, aprotinin, and pepstatin A). Protein lysates (30 μg) were boiled at 100°C in water for 5 min, separated on 4–20% SDS-PAGE gels for 2 h, transferred onto PVDF membranes at 90 v for one 1 h, blocked in 2% BSA + 5% skim milk/PBS-0.1% Tween-20 (PBS-T) for 30 min at room temperature. Primary antibodies were from Santa Cruz Biotechnology: PTHrP (sc-9680), Runx1 (sc-8563), Runx2 (sc-8566), Sox9 (sc-17340), Gata1 (sc-1234), Pax5 (sc-1974), β-catenin (sc-7199), Notch-1 (sc-6014), p16/Ink4a (M-156), β-actin (sc-1616); Abcam: Bmi-1 (ab38295); BD Biosciences: caspase-3 (CPP32); Signalway Antibody (Pearland, TX, USA): EphrinB2, GSK-3β, AKT, mTOR; R&D Systems: Wnt-5a; Cell Signaling: PARP-1 (9542); Thermo Fisher (Fremont, CA, USA): Cyclin D1 (RB212P0), P63 (MS1084P0), P21 (MS454P0). Secondary antibodies were from Santa Cruz Biotechnology.

Statistical analysis

Results are expressed as means ± SD. All data were assessed for normality by the Shapiro-Wilk method. Appropriate parametric and nonparametric testing was performed depending on data distribution. Comparisons among groups were performed with 1-way ANOVA or Kruskal-Wallis rank test depending on data distribution. Comparison between 2 groups was performed using *t* test or Mann-Whitney *U* statistic depending on data normality. Survival analysis was carried out with the Kaplan-Meier probability estimator. Significance was set at $P < 0.05$. Figures and graphics were generated with Photoshop CS3 (Adobe, San Jose, CA, USA), SigmaPlot 10.0 (Systat, Chicago, IL, USA), and Prism 4.0 (GraphPad, La Jolla, CA, USA), and statistical analysis with SigmaStat 3.5 (Systat).

RESULTS

Generation of mice lacking the midregion, NLS, and C terminus of PTHrP

A knock-in mouse lacking the sequence encoding for PTHrP–(67–137) (*Pthrp*$^{\Delta/\Delta}$), which comprises the midregion, NLS, and C terminus was engineered (Supplemental Fig. S1*A*). The presence of the mRNA for *Pthrp*$^{\Delta/\Delta}$ in bone, skin, liver, kidney, lungs, and placenta was verified by RT-PCR, and the reading frame was confirmed by sequencing (Supplemental Fig. S1*A*). The presence of PTHrP-(1–66) was demonstrated in placental tissue by Western blotting, in respiratory epithelia and skin by immunohistochemistry, and in mouse embryonic fibroblasts (MEFs) by immunocytochemistry (Supplemental Fig. S1*A, B*). PTHrP secretion was confirmed by immunoassay in conditioned medium from *Pthrp*$^{\Delta/\Delta}$ MEFs and human embryonic kidney-293 cells transfected with *Pthrp*$^{+/+}$ and *Pthrp*$^{\Delta/\Delta}$ cDNA (Supplemental Fig. S1*C*). Pups from the fifth generation onward were used for quantitative analysis.

PTHrP-(67–137) is required for growth and survival

There was no difference in body weight between *Pthrp*$^{\Delta/\Delta}$ and control pups at birth. Unlike PTHrP-knockout (*Pthrp*$^{-/-}$) pups, which died at birth (7), *Pthrp*$^{\Delta/\Delta}$ pups lived up to 20 d, but their growth rate was significantly stunted compared to controls (*Pthrp*$^{+/+}$; *Pthrp*$^{+/\Delta}$) (**Fig. 1*A***; Supplemental Fig. S2*A*), and their mortality rate was higher (Fig. 1*B*). There were no differences in fetal and placental weight, litter size, or male:female ratio (PCR to *Sry* gene), and *Pthrp*$^{\Delta/\Delta}$ pups represented ~25% of the litter (Mendelian ratio).

Lack of PTHrP-(67–137) alters skeletal and dental development

Newborn *Pthrp*$^{\Delta/\Delta}$ pups had a domed head with foreshortening of the maxilla and tongue protrusion

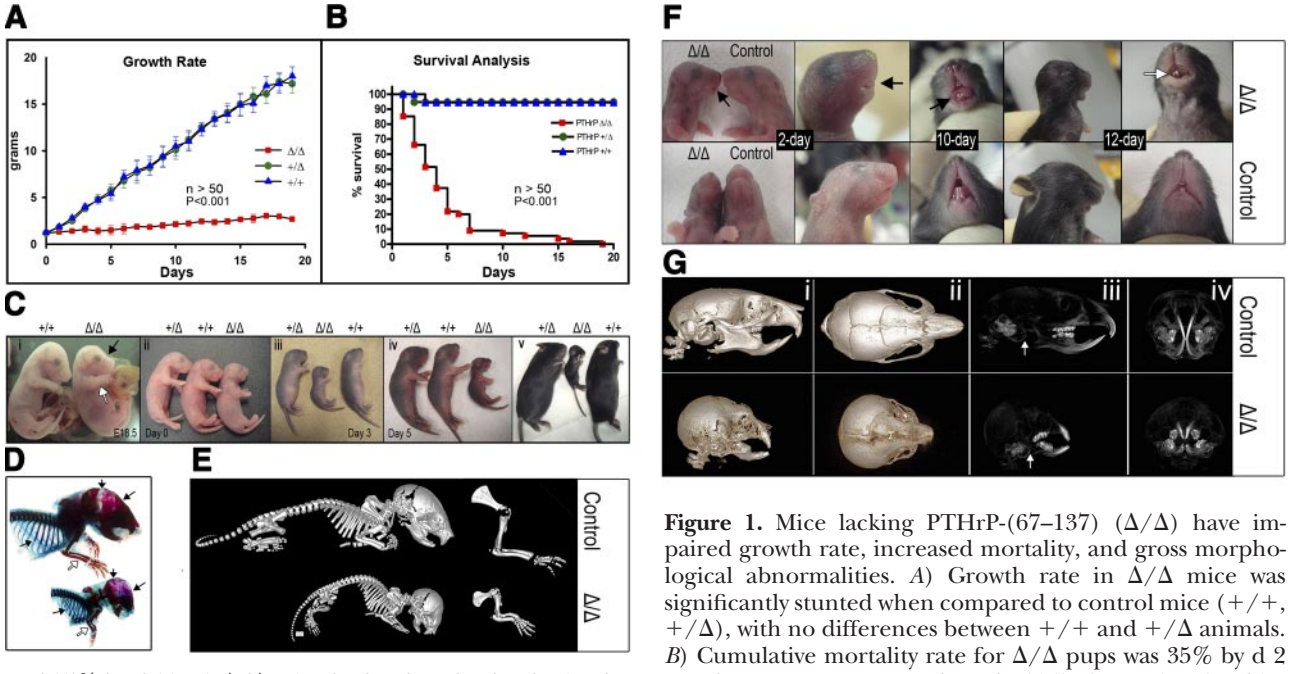

Figure 1. Mice lacking PTHrP-(67–137) (Δ/Δ) have impaired growth rate, increased mortality, and gross morphological abnormalities. *A*) Growth rate in Δ/Δ mice was significantly stunted when compared to control mice (+/+, +/Δ), with no differences between +/+ and +/Δ animals. *B*) Cumulative mortality rate for Δ/Δ pups was 35% by d 2 and 95% by d 10. *C*) Δ/Δ mice had a chondrodysplastic phenotype that was present as early as d E18.5 of gestation (*i,* white arrow), at birth (*ii*), but was clearly evident at d 3 postpartum (*iii*). Dwarfism and kyphosis were apparent in pups older than 3 d (*iii–v*). Craniofacial dysplasia with foreshortening was present as early as E18.5 (*i,* black arrow). *D*) Skeletal staining of 3-d-old Δ/Δ mice revealed less calvarial and rib mineralization (black arrows), and chondrodysplasia (white arrows). *E*) Micro-CT images of 15-d-old mice confirmed cranial dysplasia, spherical skulls, rostrocaudal facial shortening, kyphosis, and chondrodysplasia. *F*) Gross craniofacial morphology of 2- to 12-d-old Δ/Δ pups revealed a spherical skull with rostral foreshortening, tongue protrusion (black arrows), and delayed dental eruption with malaligned incisors that had a chalky discoloration (white arrow). *G*) On micro-CT, lateral, coronal, and rostral views showed morphological differences between Δ/Δ and control skulls (*i–iv*). There were differences in dental structure. Notice the proximity of the tympanic ring (white arrow) to the third molar in the Δ/Δ skull (*iii*), confirming foreshortening of the maxillae and mandible.

TABLE 1. *Microtomographic bone morphometry of the proximal tibia*

Genotype	BV/TV (%)	BS/BV (1/mm)	Tb.Th (μm)	Tb.N (1/mm)	Tb.Sp (μm)	C.Th (μm)	BMD (mg/cc)	SW/SL[a]	HW/HL[a]
Δ/Δ	18.0 ± 4.0*	115 ± 25*	19.0 ± 6.0*	8.8 ± 1.8*	100.0 ± 20.0*	60.0 ± 10.0*	139 ± 25*	0.85 ± 0.05*	0.48 ± 0.04*
+/Δ	30.0 ± 5.0	84.1 ± 12	29.0 ± 4.0	12.8 ± 0.7	60.0 ± 20.0	90.0 ± 10.0	194 ± 24	0.71 ± 0.05	0.41 ± 0.03
+/+	32.0 ± 2.0	86.2 ± 15	28.0 ± 4.0	13.8 ± 0.8	50.0 ± 20.0	100.0 ± 20.0	201 ± 28	0.73 ± .05	0.40 ± 0.03

Morphometry at d 5 (n=4). BV/TV, bone volume/total volume; BS/BV, bone surface area/bone volume; Tb.Th, trabecular thickness; Tb.N, trabecular number; Tb.Sp, trabecular spacing; C.Th, cortical wall thickness; BMD, bone mineral density; SW/SL, scapular width (cranial to caudal angles) to length ratio; HW/HL, humeral width (at the distal growth plate) to length ratio (Figure 2). [a]Higher number indicates shorter bones. *$P < 0.05$.

(craniofacial dysplasia), short limbs (hypomelia, chondrodysplasia), and a hunched back (kyphosis) (Fig. 1*C–E*). Chondrodysplasia was evident as early as E18.5 (Fig. 1*C*). The abnormal skull morphology was consistent with aberrant patterning (Fig. 1*D–F*). *Pthrp*$^{\Delta/\Delta}$ mice had less appendicular bone and skull mineralization (Fig. 1*D;* Supplemental Fig. S2*B*). Incisor eruption was delayed in *Pthrp*$^{\Delta/\Delta}$ mice (d 7 in controls *vs.* 9 in *Pthrp*$^{\Delta/\Delta}$), with incisor and molar malocclusion, malalignment, and chalky discoloration, indicating altered mineralization (Fig. 1*F*). These findings were in contrast with *Pthrp*$^{-/-}$ and *Pthrp* mice rescued with the procollagen II promoter that have failure in dental eruption (7, 28). On the basis of similar defects in humans lacking the PTH1R (10) and from the present study, it suggests that dental eruption is primarily mediated by the N terminus since tooth eruption occurred in *Pthrp*$^{\Delta/\Delta}$ animals, although it was aberrant.

To further study bone morphological and structural differences we performed micro-CT. In the proximal tibia, BV, Tb.Th, C.Th, and BMD were decreased (**Table 1**). In the skull, ratios assessing geometry were significantly different (Fig. 1*G*; **Table 2**; Supplemental Fig. S1*D*; Supplemental Videos S1 and S2). To assess microscopic features associated with the observed skeletal phenotype, we carried out bone histomorphometry and found that *Pthrp*$^{\Delta/\Delta}$ medullary cavities were redder than normal, growth plates and chondrocyte zones were shorter with chondrocyte disorientation and fewer chondrocytes per column (**Fig. 2*A–J***), less C.Th and Tb.Th (Fig. 2*H, I*), decreased osteoblast numbers (Fig. 2*K, L*), and a higher number of TRAP$^+$ cells (osteoclasts) (Fig. 2*M, N*). *Pthrp*$^{\Delta/\Delta}$ mandibles were shorter, with incisors rostrally displaced, reduced bone area, and more TRAP$^+$ cells (Fig. 2*P, Q*). Molars had altered cytodifferentiation, with irregular and disorganized odontoblasts and ameloblasts (Fig. 2*P*). The decreased bone mineralization of *Pthrp*$^{\Delta/\Delta}$ was contrary to that of *Pthrp*$^{-/-}$ mice, which had increased mineralization (7). The bone phenotype in *Pthrp*$^{\Delta/\Delta}$ mice supports the hypothesis that the midregion, NLS, and C terminus of PTHrP are critical in skeletogenesis.

Histologically, *Pthrp*$^{\Delta/\Delta}$ mice had fewer chondrocytes and osteoblasts per area (Fig. 2*K, L*), and less proliferation, based on Ki-67 immunostaining (not shown). *In vitro*, we did not find differences in chondrocyte proliferation and osteoclast differentiation, but there was less proliferation in *Pthrp*$^{\Delta/\Delta}$ osteoblasts (Fig. 2*O*). Plasma osteocalcin concentrations were lower in mutants (Supplemental Table S2). There was no evidence that *Pthrp*$^{\Delta/\Delta}$ osteoclasts had functional alterations as there were no differences in serum TRAP 5b concentrations (Supplemental Table S2).

Enteral feeding or exogenous PTHrP failed to rescue the lethal fate of *Pthrp*$^{\Delta/\Delta}$ mice

Oral gavaging of newborn pups with a milk replacer, or daily subcutaneous injections with PTHrP-(1–86), PTHrP-(1–141), and PTHrP-(67–139) (40 ng/g body weight) failed to rescue the lethal phenotype of *Pthrp*$^{\Delta/\Delta}$ mice. Treatment of calvarial osteoblasts with these PTHrP peptides (100 pM) increased their proliferation rate, but to a lesser extent than wild-type osteoblasts (Fig. 2*O*). Likewise, PTHrP peptides increased their mineralization rate, but less in *Pthrp*$^{\Delta/\Delta}$ than in wild-type osteoblasts (not shown). These results indicate that the fate of several physiological processes is determined early in development and that the effects of PTHrP on cell proliferation are primarily intracrine.

Absence of PTHrP-(67–137) impairs hematopoiesis

A major and unexpected finding in the *Pthrp*$^{\Delta/\Delta}$ bone marrow was decreased cellularity and cellular prolif-

TABLE 2. *Skull microtomography*

Genotype	OC/OI[a]	CI/OI[a]	OC/CI[a]	IT/OI[a]	IM/MO[b]	CV/OI	BMD (mg/cc)
Δ/Δ	0.75 ± 0.02*	0.88 ± 0.04*	0.85 ± 0.05	0.81 ± 0.02*	0.43 ± 0.03*	70° ± 15*	148 ± 40*
+/Δ	0.51 ± 0.04	0.66 ± 0.01	0.81 ± 0.06	0.53 ± 0.03	0.62 ± 0.05	108° ± 12°	280 ± 65
+/+	0.50 ± 0.03	0.66 ± 0.02	0.82 ± 0.06	0.52 ± 0.04	0.63 ± 0.06	112° ± 15°	275 ± 58

Microtomography at d 5 (n=4). OC/OI, occipital-coronal to occipital-incisor ratio; CI/OI, coronal-incisor to occipital incisor; OC/CI, occipital-coronal to coronal-incisor; IT/OI, intertemporal (lateral to lateral) to occipital-incisor ratio; IM/MO, incisor-molar to molar-occipital; CV/OI, cervicovertebral to occipital-incisor angle. [a]Ratios closer to 1 indicate sphere-like shape. [b]Lower numbers indicate shorter maxillae. *$P <$ 0.05.

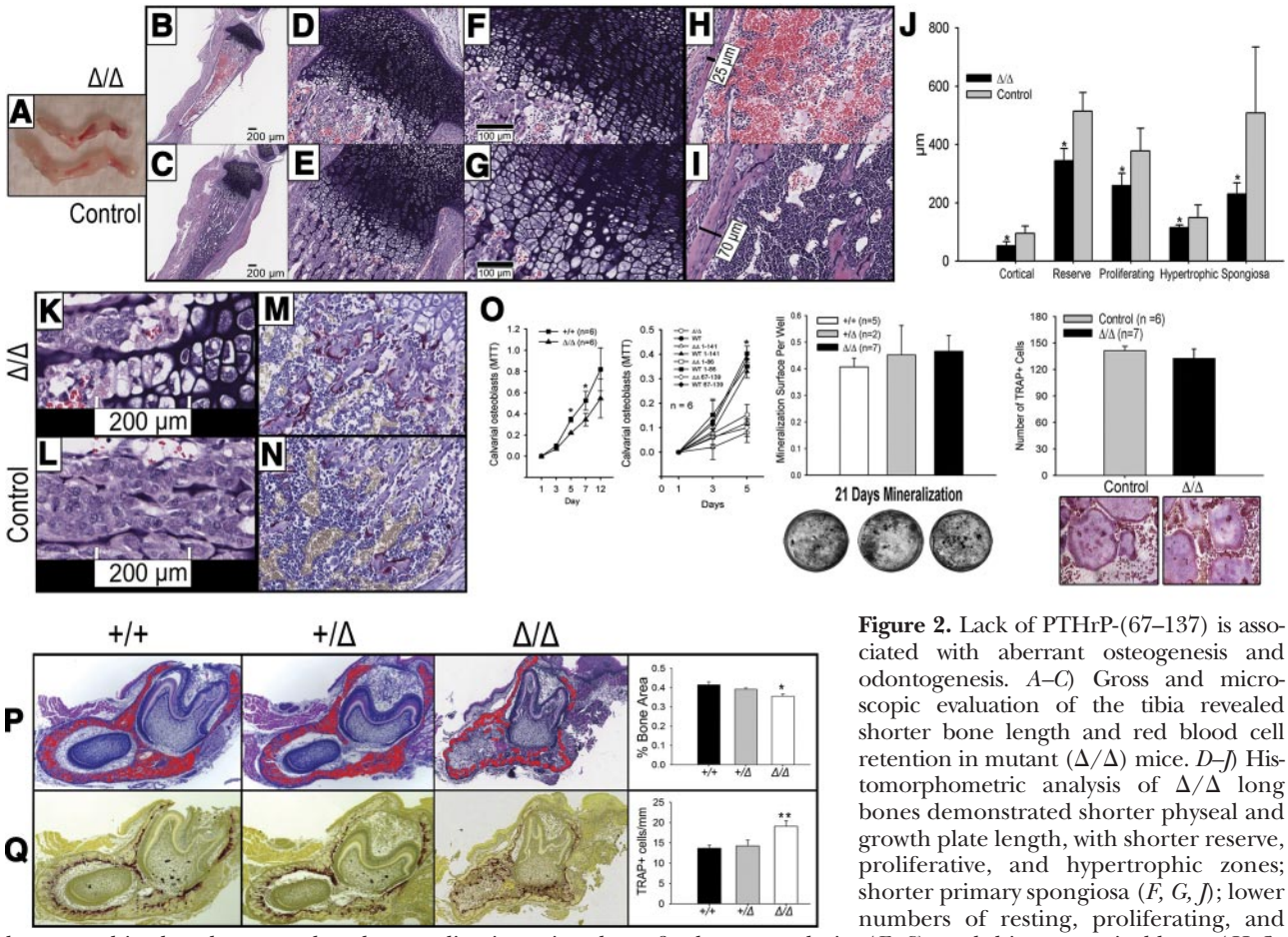

Figure 2. Lack of PTHrP-(67–137) is associated with aberrant osteogenesis and odontogenesis. *A–C*) Gross and microscopic evaluation of the tibia revealed shorter bone length and red blood cell retention in mutant (Δ/Δ) mice. *D–J*) Histomorphometric analysis of Δ/Δ long bones demonstrated shorter physeal and growth plate length, with shorter reserve, proliferative, and hypertrophic zones; shorter primary spongiosa (*F, G, J*); lower numbers of resting, proliferating, and hypertrophic chondrocytes; chondrocyte disorientation; loss of columnar polarity (*F, G*); and thinner cortical bone (*H, I*). The Δ/Δ bone marrow had decreased cellularity and lower numbers of hematopoietic precursors, and sinusoids were dilated with red blood cells (*H, I*; Supplemental Fig. S2). *K–N*) Osteoblast numbers were lower (*K, L*), while $TRAP^+$ cell numbers were higher in the Δ/Δ primary spongiosa (*M, N*). *O*) *In vitro,* Δ/Δ calvarial osteoblast proliferation was lower from d 1–7, but there was no difference in mineralization (von Kossa staining) and osteoclast differentiation (TRAP) among genotypes. Treatment with PTHrP-(1–141), PTHrP-(1–86), or PTHrP-(67–139) enhanced proliferation but to a lesser level than wild-type osteoblasts. *P*) Histology of incisors from 2- to 3-d-old mice Δ/Δ mandibles revealed flattened trabeculae, altered cytodifferentiation, abnormal cuspal formation, and decreased bone area. *Q*) Higher numbers of $TRAP^+$ cells. Values are means ± SD; $n = 6$. $^*P < 0.05$; $^{**}P < 0.01$. View: ×40.

eration (Ki-67), erythroid hypoplasia, fewer megakaryocytes/area, erythrocyte-filled sinusoids, and fewer hematopoietic precursors ($Lin^-Sca\text{-}1^+c\text{-}Kit^+$) (Figs. 2*A–C, H, I* and **3*A***, ***B***; Supplemental Fig. S2*C*). This was correlated with reduced cellularity and increased cell necrosis and apoptosis in the thymus and spleen, reduced extramedullary hematopoiesis, and decreased white and red blood cell numbers in peripheral blood (Supplemental Figs. S2*E* and S3*B, C*; Supplemental Table S2). Platelet count was lower in $Pthrp^{\Delta/\Delta}$ mice but did not reach statistical significance. There was no evidence of altered bleeding in $Pthrp^{\Delta/\Delta}$ mice. Although all genotypes showed an increase in bone marrow cellularity from birth until d 6, $Pthrp^{\Delta/\Delta}$ marrow remained less cellular (Fig. 3*A, B*; Supplemental Fig. S2*C*). The myeloid:erythroid (M:E) ratio was higher in $Pthrp^{\Delta/\Delta}$ compared to controls, with this difference becoming less apparent by d 6 (Fig. 3*B*). Day 4 $Pthrp^{\Delta/\Delta}$ bone marrow and spleen had a lower number, but a higher percentage of CD3, CD11b, and CD11c cells (Supplemental Fig. S3*A*). The percentage of B220 cells was lower in the $Pthrp^{\Delta/\Delta}$ bone marrow but higher in the $Pthrp^{\Delta/\Delta}$ spleen. IL-6 mRNA was increased in the bone marrow and calvaria of $Pthrp^{\Delta/\Delta}$ mice (Fig. 3*B*). IL-6 is a bone proresorptive cytokine that increases osteoclastogenesis. The potential role of PTHrP in hematopoiesis has not been documented before this study.

PTHrP-(67–137) is a regulator of mammary gland development

Since the absence of PTHrP or the PTH1R in mice and humans results in failure of mammary gland development (9, 10), we performed histological examination of the ventral skin of E18.5 $Pthrp^{\Delta/\Delta}$ fetuses and determined they lacked the thickened epidermal invaginations of the nipple but had a rudimentary mammary duct system (Fig. 3*C*). This confirms the N terminus of PTHrP as a key regulator of mammary development but also suggests that domains within PTHrP-(67–137) modulate mammogenesis.

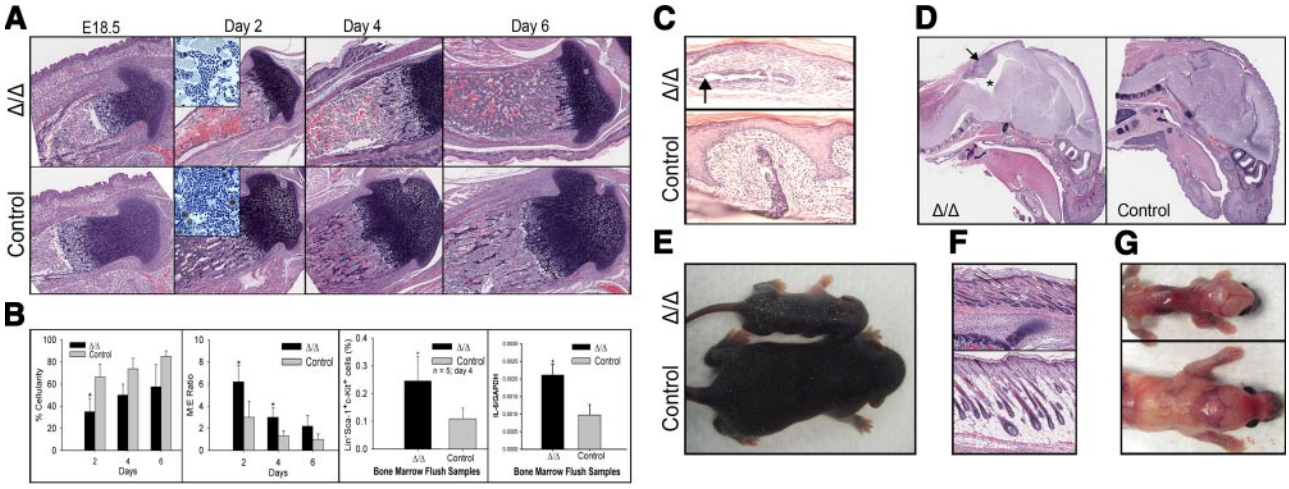

Figure 3. Absence of PTHrP-(67–137) impairs hematopoiesis, mammogenesis, brain function, and skin development. *A*) Vascular channels of Δ/Δ of E18.5 fetuses and d 2–6 pups were dilated with erythrocytes, with this difference becoming less evident by d 6. Inset: megakaryocyte (von Willebrand factor-immunopositive cell) numbers were decreased in Δ/Δ specimens. *B*) Bone marrow of 2-d-old Δ/Δ pups was less cellular and had a higher myeloid: erythroid (M:E) ratio that was less pronounced by d 6, lower numbers but a higher percentage of Lin^- $Sca\text{-}1^+$ $c\text{-}Kit^+$ hematopoietic stem cells, and higher Il-6 mRNA expression. *C*) Mammary gland histology revealed that Δ/Δ fetuses lacked the epidermal changes that characterize nipple morphogenesis observed in control fetuses; however, mammary ducts were observed in Δ/Δ fetuses (black arrow; ×100). *D*) A number of Δ/Δ brains had cerebellar herniation (arrow) and hydrocephalus (asterisk), which likely was associated with the intention tremors (Supplemental Video S3) observed in these mice (×20). *E, F*) Δ/Δ pups older than 3 d of age had marked seborrhea sicca (E), which histologically revealed epidermal and follicular basket-weave to compact hyperkeratosis (F). *G*) Δ/Δ pups had subcutaneous and visceral adipose tissue depletion that was evident on histological examination (5-d-old mice). Values are means ± SD. $^*P < 0.05$.

PTHrP-(67–137) deficiency affects other body systems

$Pthrp^{\Delta/\Delta}$ pups that lived past d 7 developed intention tremors consistent with cerebellar dysfunction (Supplemental Video S3). A number of these pups had hydrocephalus and cerebellar herniation through the foramen magnum (Fig. 3*D*), likely from cranial malformation. These signs could have also resulted from a lack of neuroprotection from PTHrP, as $Pthrp^{-/-}$ brains are more susceptible to neuroexcitation (29). Of interest, there was more TUNEL labeling and less Ki-67 immunostaining in $Pthrp^{\Delta/\Delta}$ brains (Supplemental Fig. S2*D, E*). No macroscopic or histological epidermal or dermal abnormalities were seen in $Pthrp^{\Delta/\Delta}$ E18.5 fetuses or newborn pups; however, by d 3, generalized marked seborrhea sicca developed (Fig. 3*E*). This clinical appearance was evident histologically as epidermal and follicular basket-weave to compact hyperkeratosis (Fig. 3*F*).

At birth, no gross differences in subcutaneous or visceral adipose tissue were found; however, by d 1, $Pthrp^{\Delta/\Delta}$ pups had signs of decreased dietary intake or defective energy metabolism, including adipose tissue and hepatocyte glycogen depletion (Fig. 3*F, G*; Supplemental Fig. S3*B*), hypoglycemia, hypotriglyceridemia, and hypoinsulinemia (Supplemental Table S2). We further observed that pancreatic islet cell numbers and insulin immunostaining were decreased (not shown), and serum insulin concentrations were lower (Supplemental Table S2). Our findings indicate that PTHrP participates in the energy metabolism and are further supported by studies showing that PTHrP regulates pancreatic β-cell function (22, 30).

No differences in the parathyroid, pituitary, and adrenal glands were found. Because $Pthrp^{\Delta/\Delta}$ E18.5 fetuses and 0- to 6-d-old pups had hypocalcemia, we measured serum PTH and PTHrP concentrations, with no differences found (Supplemental Table S2). We speculate that the lack of midregion PTHrP, which has been implicated in transepithelial calcium transport (12, 13) may be responsible for hypocalcemia in $Pthrp^{\Delta/\Delta}$ mice. There is limited information on PTHrP and intestinal calcium absorption (31); however, PTHrP concentrations are >1000-fold higher in milk than in blood (32).

PTHrP-(67–137) is a regulator of programmed cell death

Since it has been proposed that the NLS of PTHrP reduces apoptosis (14, 15, 19), TUNEL labeling, caspase-3 immunostaining, and PARP-1 immunoblotting were performed, and we found higher apoptotic rates in $Pthrp^{\Delta/\Delta}$ chondrocytes, splenocytes, thymocytes, bone marrow, and brain (Supplemental Figs. S2*D, E* and S3*C*). We also determined by flow cytometry that camptothecin-treated primary chondrocytes had higher apoptotic rates (Supplemental Fig. S3*D*). These findings support that PTHrP-(67–137) has *in vivo* antiapoptotic functions.

Absence of PTHrP-(67–137) alters skeletal and hematopoietic gene expression

The abnormal skeletal phenotype of $Pthrp^{\Delta/\Delta}$ mice prompted us to assess the mRNA expression of genes involved in osteogenesis, chondrogenesis, and apoptosis in the tibial metaphysis and calvariae of 2-d-old mice

using PCR arrays. The following genes were further evaluated by quantitative real-time PCR: *Ocn, Runx2, Ihh, Sox9, Fgf1, Fgf3, tuftelin1, Itga3,* β*-catenin, ephrinB2, EphB4, Crtl1, PPAR*γ, *Bcl2,* and *P63.* To address the abnormal hematopoietic phenotype, selected hematopoietic genes (*Runx1, Gata1, PU.1, C/EBP,* and *Pax5*) were evaluated in the bone marrow. In the *Pthrp*$^{\Delta/\Delta}$ metaphysis *Runx2, Ocn, Sox9, Crtl1,* β*-catenin, EphrinB2,* and *Bcl2* were underexpressed, while *Ffg3, Ihh, Itga3, and Il-6* were overexpressed (**Fig. 4*A***). In the bone marrow, *Runx1, Gata1, PU.1,* and *Pax5* were underexpressed (Fig. 4*A*). In the calvariae, *Ocn* and *Crtl1* were underexpressed, while *Fgf3, Ihh, Il-6, and P63* were overexpressed (Supplemental Fig. S3*E*). There were no differences in *Pthrp, Pth1r, or PPAR*γ mRNA expression (Fig. 4*A*). The underexpression of *Runx2, Runx1, Sox9, EphrinB2,* β*-catenin, Gata1,* and *Pax5* was supported by less protein detection on Western blots of tibial protein extracts (Fig. 4*B*). In addition, there was more GSK-*3*β, *P16/Ink4a,* and less β*-catenin* protein in the *Pthrp*$^{\Delta/\Delta}$ bone samples. The abnormal gene expression and protein patterns in *Pthrp*$^{\Delta/\Delta}$ mice were consistent with the abnormal skeletogenesis, decreased hematopoiesis, and increased apoptosis observed, supporting PTHrP as an important factor in cell fate.

A model for the role of PTHrP-(67–137) in skeletogenesis and hematopoiesis

On the basis of the findings presented in this study, we propose that in the bone and bone marrow compartments PTHrP-(67–137) is necessary for the commitment of mesenchymal and hematopoietic precursors to their respective mature lineages (**Fig. 5**). Specifically, the decreased osteoblast and chondrocyte numbers and low plasma osteocalcin concentrations, together with the underexpression of *Runx2, Sox9, EphrinB2, Crtl1,* β*-catenin,* and *cyclin D1,* and overexpression of *GSK-3*β and *P16/Ink4a* indicate that PTHrP-(67–137) is a regulator of this step in cellular development (Fig. 5*A*). Likewise, the decreased numbers of hematopoietic precursors ($Lin^{-}Sca\text{-}1^{+}c\text{-}Kit^{+}$), bone marrow hypocellularity, and decreased *Runx1, Gata1, Pax5,* and *PU.1* mRNA expression in *Pthrp*$^{\Delta/\Delta}$ mice suggest that PTHrP is important in hematopoiesis (Fig. 5*B*). The dysregulation of genes involved in apoptosis and aging (*GSK-3*β*, P16/Ink4a,* β*-catenin, P63, Bcl-2, mTOR*) supports PTHrP as a regulator of these processes (Fig. 5*C*).

DISCUSSION

The biological functions of PTHrP on morphogenesis have been attributed to its N terminus (7). Previous studies suggesting that PTHrP has other domains with biological functions (12, 13, 15, 18, 20, 33) prompted us to generate a knock-in mouse lacking the midregion, NLS, and C terminus of PTHrP. Here, we show that indeed, these domains of PTHrP are essential for development and survival, strengthening the hypothesis that many of the actions attributed to the N terminus of PTHrP are mediated by regions within PTHrP-(67–137), but also that these functions are paracrine, autocrine, and intracrine in nature. This is further supported by the fact that daily injections of PTHrP failed to rescue the lethal phenotype of *Pthrp*$^{\Delta/\Delta}$ mice.

Although PTH-(1–34) and PTHrP-(1–36) are equipotent through the PTH1R in rodents (34), it remains unclear whether the absence of the NLS or C terminus impairs the N-terminal interaction with this or other

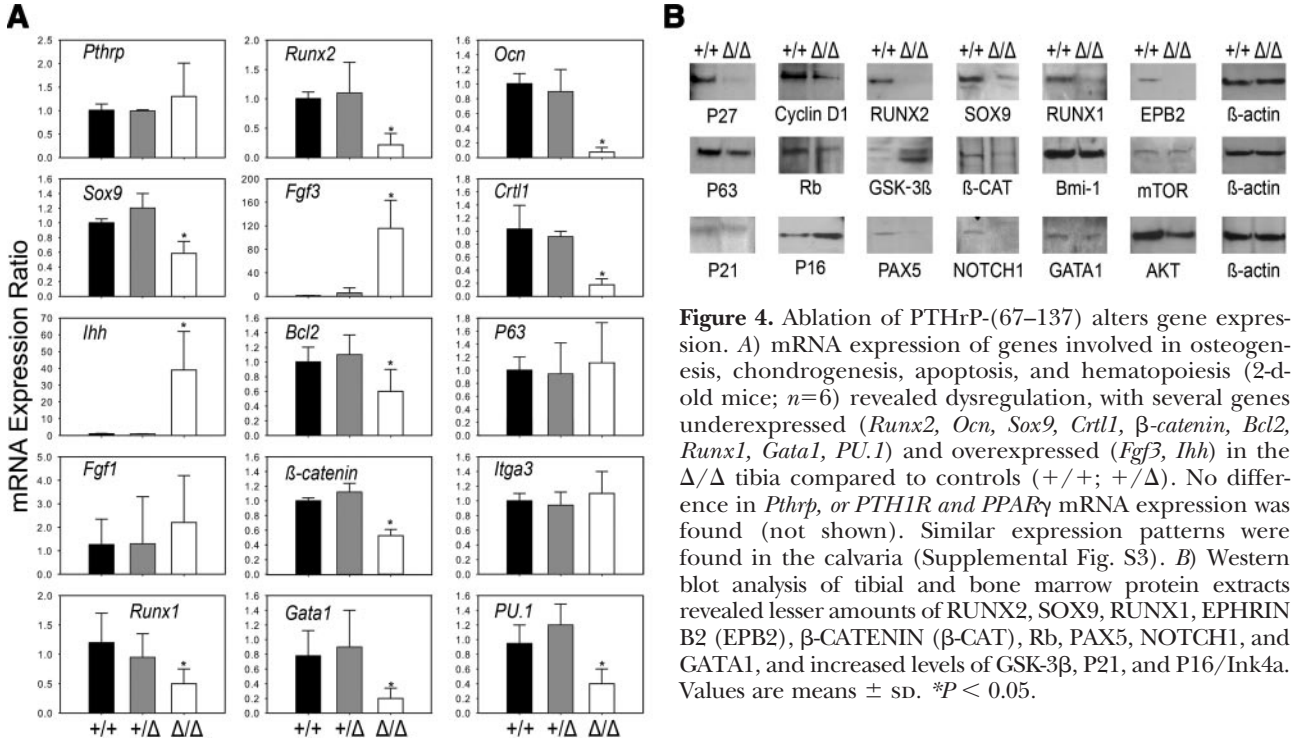

Figure 4. Ablation of PTHrP-(67–137) alters gene expression. *A*) mRNA expression of genes involved in osteogenesis, chondrogenesis, apoptosis, and hematopoiesis (2-d-old mice; $n=6$) revealed dysregulation, with several genes underexpressed (*Runx2, Ocn, Sox9, Crtl1,* β*-catenin, Bcl2, Runx1, Gata1, PU.1*) and overexpressed (*Fgf3, Ihh*) in the Δ/Δ tibia compared to controls (+/+; +/Δ). No difference in *Pthrp, or PTH1R and PPAR*γ mRNA expression was found (not shown). Similar expression patterns were found in the calvaria (Supplemental Fig. S3). *B*) Western blot analysis of tibial and bone marrow protein extracts revealed lesser amounts of RUNX2, SOX9, RUNX1, EPHRIN B2 (EPB2), β-CATENIN (β-CAT), Rb, PAX5, NOTCH1, and GATA1, and increased levels of GSK-3β, P21, and P16/Ink4a. Values are means ± SD. $^{*}P < 0.05$.

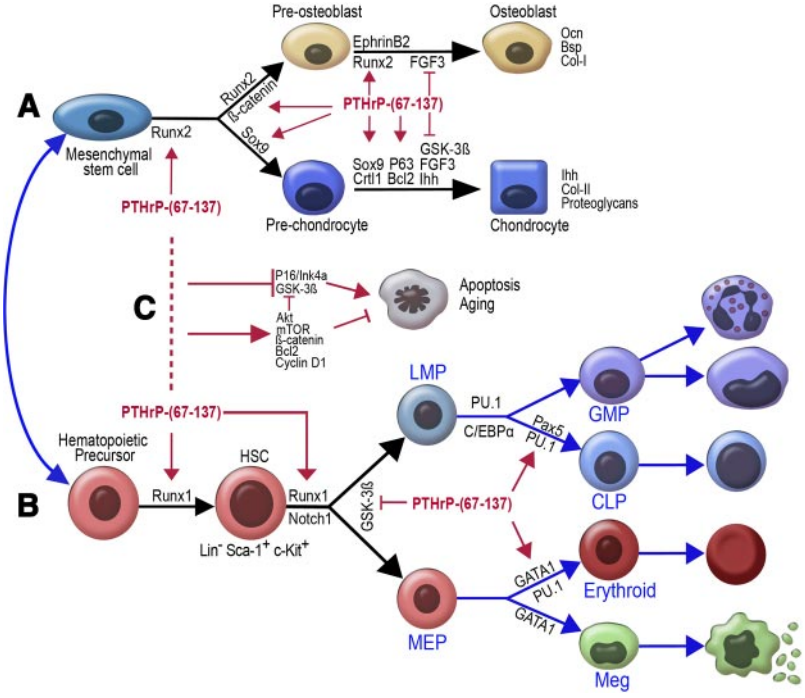

Figure 5. Model for the role of PTHrP-(67–137) in skeletogenesis and hematopoiesis. *A*) The work presented here indicates that PTHrP-(67–137) increases *Runx2* mRNA expression to lead mesenchymal stem cells to the osteogenic and chondrogenic lineages. By inducing *Sox9* mRNA expression in the epiphyses and metaphyses, PTHrP commits stem cells to chondrogenesis, while in the diaphysis, PTHrP-driven mRNA expression of *Runx2* commits stem cells to osteogenesis. PTHrP-(67–137) also regulates other important skeletogenic genes (β-*catenin, Ihh, Fgf3, Crtl1, ephrin B2*) (Fig. 4*A*). *B*) Underexpression of *Runx1* and *Notch1*, which are required for hematopoiesis, and underexpression of *PU.1, Pax5,* and *Gata1,* which are necessary for further hematopoietic differentiation, links PTHrP to functions not previously described. It also suggests that PTHrP participates in the communication between the bone/bone marrow compartments. *C*) Dysregulation of genes involved in apoptosis and aging (*GSK-3*β, *P16/Ink4a, P21,* β-*catenin, P63, Bcl-2*) supports PTHrP as a regulator of these processes. HSC, hematopoietic stem cell; LMP, lymphoid-myeloid progenitor; GMP, granulocyte-monocyte progenitor; CLP, common lymphoid progenitor; MEP, megakaryocyte-erythroid progenitor; Meg, megakaryocyte.

receptors. While speculative, this could be accepted as a potential explanation for the abnormal phenotype of *Pthrp*$^{\Delta/\Delta}$ mice, which may represent a hypomorphic form of the *Pthrp*$^{-/-}$ phenotype (7). However, we believe that these effects are independent of the N terminus, mediated at the intracrine level by the NLS and at the autocrine and paracrine level by cell membrane receptors for the C terminus of PTHrP. Cell culture studies have shown that the NLS of PTHrP associates with importin β and GTP-Ran to promote its translocation into the nucleus (16, 17), where it interacts with RNA (14, 19) to reduce apoptosis (15). Likewise, other investigators have shown that the midregion and C terminus of PTHrP interact with cell surface receptors to increase intracellular cAMP and calcium concentrations (35–37); however, the structure of these receptors remains unknown. One might speculate that the increased osteoclast number in the trabeculae of *Pthrp*$^{\Delta/\Delta}$ mice could have resulted from the absence of PTHrP-(107–111), also known as osteostatin, which inhibits osteoclastic activity (33), while the decreased proliferation and increased apoptosis could also been a consequence of C-terminal and midregion deletion, both of which have been shown to promote cell proliferation (18, 37, 38).

Pthrp$^{\Delta/\Delta}$ mice have a similar gross appearance to the *Pthrp*$^{-/-}$ mice (7); however, *Pthrp*$^{-/-}$ pups die within minutes of birth with evidence of cyanosis and respiratory failure (7), while *Pthrp*$^{\Delta/\Delta}$ pups appear normal at birth, with most of them dying after d 3. Since *Pth1r*$^{-/-}$ fetuses die earlier in development than *Pthrp*$^{-/-}$ fetuses (7, 39); this indicates that the ontogenic functions of the N terminus of PTHrP occur earlier in development and further substantiates our findings that PTHrP has functions not mediated by this receptor. Of interest, mice lacking the cartilage linking protein 1 (*Crtl1*$^{-/-}$; *Hapln1*$^{-/-}$) (40) had a similar phenotype to *Pthrp*$^{\Delta/\Delta}$ and *Pthrp*$^{-/-}$ pups, including abnormal craniofacial development, chondrodysplasia and dwarfism. However, unlike *Pthrp*$^{\Delta/\Delta}$ mutants, but similar to *Pthrp*$^{-/-}$ pups, *Crtl1*$^{-/-}$ die at birth from respiratory failure (7, 40). The decreased mRNA expression of *Crtl1* and its regulator, *Sox9,* suggests direct and indirect interactions between PTHrP and CRTL1 (HAPLN1) (41). We also believe that *P63* and *P16/Ink4a*, which were deregulated, are central to the *Pthrp*$^{\Delta/\Delta}$ phenotype. P63 is a p53-related protein that regulates morphogenesis and senescence, and *P63*$^{-/-}$ mice have aberrant skeletogenesis, hyperkeratosis, and short life span (42, 43).

Skeletal mineralization was reduced in *Pthrp*$^{\Delta/\Delta}$ mice, which is in contrast with the increased and premature ossification observed in *Pthrp*$^{-/-}$ mice (7), indicating that PTHrP-(67–137) regulates skeletal development differently than the N terminus. It also shows that PTHrP-(67–137) has essential roles in the commitment of stromal cells to the skeletogenic lineage, as documented by the underexpression of *Runx2, Ocn, Sox9, EphrinB2,* β-*catenin,* and *Crtl1,* and overexpression *of Fgf3, Ihh,* and *GSK-3*β. Sox9 and *Runx2* are the master transcription factors for chondrogenesis and osteogenesis, respectively. The overexpression of *Ihh, Fgf3, and GSK-3*β in *Pthrp*$^{\Delta/\Delta}$ mice supports PTHrP as an inhibitor of these factors, but also that this inhibition is independent of PTH1R signaling (44). We believe that enhanced *Fgf3* expression contributed in part to abnormal skeletal morphogenesis of *Pthrp*$^{\Delta/\Delta}$ mice as fibroblast growth factor (FGF) 3 is a negative regulator of chondrocyte proliferation and bone growth, gain-of-function mutations of the FGF receptors are responsible for most forms of human chondrodysplasias (44), and mice overexpressing FGFR3 have skeletal phenotypical similarities to that of *Pthrp*$^{\Delta/\Delta}$ mice (45, 46). On the basis of these findings, we propose that a lack of stromal cell commitment is central to the skeletal phenotype ob-

served in *Pthrp*$^{\Delta/\Delta}$ mice, as osteoblast and chondrocyte number was decreased in skeletal tissue. The low chondrocyte number and disorganization in *Pthrp*$^{\Delta/\Delta}$ mice demonstrates that the paracrine effects of PTHrP are dependent on post-transcriptional modifications of PTHrP, expression of distinct PTHrP receptors, or intracrine functions, reinforcing the theory of alternative PTH1R ligands, and/or PTHrP signaling pathways (36, 47). The fact that mice expressing PTHrP-(1–84) (26) show less severe skeletal abnormalities than *Pthrp*$^{\Delta/\Delta}$ mice, with apparently normal hematopoiesis supports distinct functions for the midregion of PTHrP.

The discovery that *Pthrp*$^{\Delta/\Delta}$ mice had defective hematopoiesis raises important questions on the role of PTHrP in the communication between osteogenic and hematopoietic precursors, regulation of bone mass, and hematopoiesis. Since constitutive expression of the PTH1R in murine osteogenic cells delays hematopoiesis (48), this implies that there are complementary actions among the different domains of PTHrP, and likely PTH, within the bone and bone marrow compartments. It remains to be elucidated whether the effects of PTHrP-(67–137) on osteoblasts and hematopoietic cells are direct or the result of intercellular communications in the bone microenvironment.

It is unclear why *Pthrp*$^{\Delta/\Delta}$ pups failed to thrive, but it could relate to an inability to nurse from craniofacial malformation, dental malocclusion, tongue protrusion, as well as dysregulated energy metabolism. Endocrine dysregulation is possible as enteral feeding did not rescue *Pthrp*$^{\Delta/\Delta}$ mice, which also had low insulin concentrations. It has been reported that PTHrP regulates insulin secretion by pancreatic β cells (22, 30). The fact that the nipples from *Pthrp*$^{\Delta/\Delta}$ pups lacked the typical epidermal invaginations, but had a rudimentary mammary duct system, suggests that PTHrP-(67–137) is not required for mammary mesenchyme formation. PTHrP is an important mediator of epithelial–mesenchymal interactions since humans and mice lacking PTHrP or the PTH1R have a failure of embryonic mammary gland development due to a defect in mammary mesenchyme differentiation (9, 10). These effects might be, in part, mediated by P63 as inactivating mutations of P63 in humans are associated with mammary gland aplasia (49).

In summary, the midregion, NLS, and C terminus of PTHrP are essential for survival. The presence of skeletal, hematopoietic, and lethal phenotypes in *Pthrp*$^{\Delta/\Delta}$ mice supports the hypothesis that PTHrP is pleiotropic, and its biological actions are mediated by receptors other than the PTH1R. It also indicates that the specificity of PTHrP to various targets results from tissue-specific modifications leading to autocrine, paracrine, and intracrine functions. FJ

The authors thank laboratory members for their support; Hui Wang and Gustavo Leone (Human Cancer Genetics Program, The Ohio State University, Columbus, OH, USA) for their assistance with embryonic stem cell work and for providing the *EIIa-Cre* mice; Sanjay Singh and Girish Rajgolikar for technical assistance; Jan Hu for consultation regarding tooth morphology; and Alan Flechtner and Florinda Jaynes for histological specimen processing. The *pPNT* plasmid was a kind gift from Dr. Michael Weinstein (Human Cancer Genetics Program, The Ohio State University). The authors thank Dr. T. J. Martin for the constructive comments on this manuscript. This study was possible with funding from the National Institutes of Health to R.E.T. (K01 RR018924; S10 RR020888) and L.K.M. (DE014073 and CA09390). The authors declare no competing financial interests.

REFERENCES

1. Moseley, J. M., Kubota, M., Diefenbach-Jagger, H., Wettenhall, R. E., Kemp, B. E., Suva, L. J., Rodda, C. P., Ebeling, P. R., Hudson, P. J., and Zajac, J. D. (1987) Parathyroid hormone-related protein purified from a human lung cancer cell line. *Proc. Natl. Acad. Sci. U. S. A.* **84,** 5048–5052
2. Suva, L. J., Winslow, G. A., Wettenhall, R. E., Hammonds, R. G., Moseley, J. M., Diefenbach-Jagger, H., Rodda, C. P., Kemp, B. E., Rodriguez, H., and Chen, E. Y. (1987) A parathyroid hormone-related protein implicated in malignant hypercalcemia: cloning and expression. *Science* **237,** 893–896
3. Martin, T. J., Ebeling, P. R., Rodda, C. P., and Kemp, B. E. (1988) Humoral hypercalcemia of malignancy: involvement of a novel hormone. *Aust. N. Z. J. Med.* **18,** 287–295
4. Wysolmerski, J. J., and Stewart, A. F. (1998) The physiology of parathyroid hormone-related protein: an emerging role as a developmental factor. *Annu. Rev. Physiol.* **60,** 431–460
5. Strewler, G. J., Stern, P. H., Jacobs, J. W., Eveloff, J., Klein, R. F., Leung, S. C., Rosenblatt, M., and Nissenson, R. A. (1987) Parathyroid hormonelike protein from human renal carcinoma cells. Structural and functional homology with parathyroid hormone. *J. Clin. Invest.* **80,** 1803–1807
6. Weir, E. C., Philbrick, W. M., Amling, M., Neff, L. A., Baron, R., and Broadus, A. E. (1996) Targeted overexpression of parathyroid hormone-related peptide in chondrocytes causes chondrodysplasia and delayed endochondral bone formation. *Proc. Natl. Acad. Sci. U. S. A.* **93,** 10240–10245
7. Karaplis, A. C., Luz, A., Glowacki, J., Bronson, R. T., Tybulewicz, V. L., Kronenberg, H. M., and Mulligan, R. C. (1994) Lethal skeletal dysplasia from targeted disruption of the parathyroid hormone-related peptide gene. *Genes Dev.* **8,** 277–289
8. Lee, K., Lanske, B., Karaplis, A. C., Deeds, J. D., Kohno, H., Nissenson, R. A., Kronenberg, H. M., and Segre, G. V. (1996) Parathyroid hormone-related peptide delays terminal differentiation of chondrocytes during endochondral bone development. *Endocrinology* **137,** 5109–5118
9. Wysolmerski, J. J., Philbrick, W. M., Dunbar, M. E., Lanske, B., Kronenberg, H., and Broadus, A. E. (1998) Rescue of the parathyroid hormone-related protein knockout mouse demonstrates that parathyroid hormone-related protein is essential for mammary gland development. *Development* **125,** 1285–1294
10. Wysolmerski, J. J., Cormier, S., Philbrick, W. M., Dann, P., Zhang, J. P., Roume, J., Delezoide, A. L., and Silve, C. (2001) Absence of functional type 1 parathyroid hormone (PTH)/PTH-related protein receptors in humans is associated with abnormal breast development and tooth impaction. *J. Clin. Endocrinol. Metab.* **86,** 1788–1794
11. VanHouten, J. N., Dann, P., Stewart, A. F., Watson, C. J., Pollak, M., Karaplis, A. C., and Wysolmerski, J. J. (2003) Mammary-specific deletion of parathyroid hormone-related protein preserves bone mass during lactation. *J. Clin. Invest.* **112,** 1429–1436
12. Care, A. D., Abbas, S. K., Pickard, D. W., Barri, M., Drinkhill, M., Findlay, J. B., White, I. R., and Caple, I. W. (1990) Stimulation of ovine placental transport of calcium and magnesium by mid-molecule fragments of human parathyroid hormone-related protein. *Exp. Physiol.* **75,** 605–608
13. Wu, T. L., Vasavada, R. C., Yang, K., Massfelder, T., Ganz, M., Abbas, S. K., Care, A. D., and Stewart, A. F. (1996) Structural and physiologic characterization of the mid-region secretory species of parathyroid hormone-related protein. *J. Biol. Chem.* **271,** 24371–24381
14. Aarts, M. M., Davidson, D., Corluka, A., Petroulakis, E., Guo, J., Bringhurst, F. R., Galipeau, J., and Henderson, J. E. (2001) Parathyroid hormone-related protein promotes quiescence and

survival of serum-deprived chondrocytes by inhibiting rRNA synthesis. *J. Biol. Chem.* **276,** 37934–37943
15. Henderson, J. E., Amizuka, N., Warshawsky, H., Biasotto, D., Lanske, B. M., Goltzman, D., and Karaplis, A. C. (1995) Nucleolar localization of parathyroid hormone-related peptide enhances survival of chondrocytes under conditions that promote apoptotic cell death. *Mol. Cell. Biol.* **15,** 4064–4075
16. Lam, M. H., Briggs, L. J., Hu, W., Martin, T. J., Gillespie, M. T., and Jans, D. A. (1999) Importin beta recognizes parathyroid hormone-related protein with high affinity and mediates its nuclear import in the absence of importin alpha. *J. Biol. Chem.* **274,** 7391–7398
17. Lam, M. H., Hu, W., Xiao, C. Y., Gillespie, M. T., and Jans, D. A. (2001) Molecular dissection of the importin beta1-recognized nuclear targeting signal of parathyroid hormone-related protein. *Biochem. Biophys. Res. Commun.* **282,** 629–634
18. De Miguel, F., Fiaschi-Taesch, N., Lopez-Talavera, J. C., Takane, K. K., Massfelder, T., Helwig, J. J., and Stewart, A. F. (2001) The C-terminal region of PTHrP, in addition to the nuclear localization signal, is essential for the intracrine stimulation of proliferation in vascular smooth muscle cells. *Endocrinology* **142,** 4096–4105
19. Aarts, M. M., Levy, D., He, B., Stregger, S., Chen, T., Richard, S., and Henderson, J. E. (1999) Parathyroid hormone-related protein interacts with RNA. *J. Biol. Chem.* **274,** 4832–4838
20. Aarts, M. M., Rix, A., Guo, J., Bringhurst, R., and Henderson, J. E. (1999) The nucleolar targeting signal (NTS) of parathyroid hormone related protein mediates endocytosis and nucleolar translocation. *J. Bone Miner. Res.* **14,** 1493–1503
21. Pache, J. C., Burton, D. W., Deftos, L. J., and Hastings, R. H. (2006) A carboxyl leucine-rich region of parathyroid hormone-related protein is critical for nuclear export. *Endocrinology* **147,** 990–998
22. Sawada, Y., Zhang, B., Okajima, F., Izumi, T., and Takeuchi, T. (2001) PTHrP increases pancreatic beta-cell-specific functions in well-differentiated cells. *Mol. Cell. Endocrinol.* **182,** 265–275
23. Burtis, W. J., Fodero, J. P., Gaich, G., Debeyssey, M., and Stewart, A. F. (1992) Preliminary characterization of circulating amino- and carboxy-terminal fragments of parathyroid hormone-related peptide in humoral hypercalcemia of malignancy. *J. Clin. Endocrinol. Metab.* **75,** 1110–1114
24. Burtis, W. J., Dann, P., Gaich, G. A., and Soifer, N. E. (1994) A high abundance midregion species of parathyroid hormone-related protein: immunological and chromatographic characterization in plasma. *J. Clin. Endocrinol. Metab.* **78,** 317–322
25. Uemura, H., Yasui, T., Yoneda, N., Irahara, M., and Aono, T. (1997) Measurement of N- and C-terminal-region fragments of parathyroid hormone-related peptide in milk from lactating women and investigation of the relationship of their concentrations to calcium in milk. *J. Endocrinol.* **153,** 445–451
26. Miao, D., Su, H., He, B., Gao, J., Xia, Q., Zhu, M., Gu, Z., Goltzman, D., and Karaplis, A. C. (2008) Severe growth retardation and early lethality in mice lacking the nuclear localization sequence and C-terminus of PTH-related protein. *Proc. Natl. Acad. Sci. U. S. A.* **105,** 20309–20314
27. Vandesompele, J., De, P. K., Pattyn, F., Poppe, B., Van, R. N., De, P. A., and Speleman, F. (2002) Accurate normalization of real-time quantitative RT-PCR data by geometric averaging of multiple internal control genes. *Genome Biol.* **3,** RESEARCH0034
28. Philbrick, W. M., Dreyer, B. E., Nakchbandi, I. A., and Karaplis, A. C. (1998) Parathyroid hormone-related protein is required for tooth eruption. *Proc. Natl. Acad. Sci. U. S. A.* **95,** 11846–11851
29. Chatterjee, O., Nakchbandi, I. A., Philbrick, W. M., Dreyer, B. E., Zhang, J. P., Kaczmarek, L. K., Brines, M. L., and Broadus, A. E. (2002) Endogenous parathyroid hormone-related protein functions as a neuroprotective agent. *Brain Res.* **930,** 58–66
30. Cebrian, A., Garcia-Ocana, A., Takane, K. K., Sipula, D., Stewart, A. F., and Vasavada, R. C. (2002) Overexpression of parathyroid hormone-related protein inhibits pancreatic beta-cell death in vivo and in vitro. *Diabetes* **51,** 3003–3013
31. Fuentes, J., Figueiredo, J., Power, D. M., and Canario, A. V. (2006) Parathyroid hormone-related protein regulates intestinal calcium transport in sea bream (*Sparus auratus*). *Am. J. Physiol.* **291,** R1499–R1506
32. Onda, K., Sato, A., Yamaguchi, M., Matsuki, N., Ono, K., and Wada, Y. (2006) Parathyroid hormone-related protein (PTHrP) and Ca levels in the milk of lactating cows. *J. Vet. Med. Sci.* **68,** 709–713
33. Fenton, A. J., Kemp, B. E., Hammonds, R. G., Jr., Mitchelhill, K., Moseley, J. M., Martin, T. J., and Nicholson, G. C. (1991) A potent inhibitor of osteoclastic bone resorption within a highly conserved pentapeptide region of parathyroid hormone-related protein; PTHrP[107–111]. *Endocrinology* **129,** 3424–3426
34. Lopez-Hilker, S., Martin, K. J., Sugimoto, T., and Slatopolsky, E. (1992) Biologic activities of parathyroid hormone (1–34) and parathyroid hormone-related peptide (1–34) in isolated perfused rat femur. *J. Lab. Clin. Med.* **119,** 738–743
35. Seitz, P. K., Zhang, R. W., Simmons, D. J., and Cooper, C. W. (1995) Effects of C-terminal parathyroid hormone-related peptide on osteoblasts. *Miner. Electrolyte. Metab.* **21,** 180–183
36. Valin, A., Guillen, C., and Esbrit, P. (2001) C-terminal parathyroid hormone-related protein (PTHrP) (107–139) stimulates intracellular Ca^{2+} through a receptor different from the type 1 PTH/PTHrP receptor in osteoblastic osteosarcoma UMR 106 cells. *Endocrinology* **142,** 2752–2759
37. Orloff, J. J., Ganz, M. B., Nathanson, M. H., Moyer, M. S., Kats, Y., Mitnick, M., Behal, A., Gasalla-Herraiz, J., and Isales, C. M. (1996) A midregion parathyroid hormone-related peptide mobilizes cytosolic calcium and stimulates formation of inositol trisphosphate in a squamous carcinoma cell line. *Endocrinology* **137,** 5376–5385
38. De Gortazar, A. R., Alonso, V., Alvarez-Arroyo, M. V., and Esbrit, P. (2006) Transient exposure to PTHrP (107–139) exerts anabolic effects through vascular endothelial growth factor receptor 2 in human osteoblastic cells in vitro. *Calcif. Tissue Int.* **79,** 360–369
39. Lanske, B., Karaplis, A. C., Lee, K., Luz, A., Vortkamp, A., Pirro, A., Karperien, M., Defize, L. H., Ho, C., Mulligan, R. C., Abou-Samra, A. B., Juppner, H., Segre, G. V., and Kronenberg, H. M. (1996) PTH/PTHrP receptor in early development and Indian hedgehog-regulated bone growth. *Science* **273,** 663–666
40. Watanabe, H., and Yamada, Y. (1999) Mice lacking link protein develop dwarfism and craniofacial abnormalities. *Nat. Genet.* **21,** 225–229
41. Kou, I., and Ikegawa, S. (2004) SOX9-dependent and -independent transcriptional regulation of human cartilage link protein. *J. Biol. Chem.* **279,** 50942–50948
42. Keyes, W. M., Wu, Y., Vogel, H., Guo, X., Lowe, S. W., and Mills, A. A. (2005) p63 deficiency activates a program of cellular senescence and leads to accelerated aging. *Genes Dev.* **19,** 1986–1999
43. Su, X., Cho, M. S., Gi, Y. J., Ayanga, B. A., Sherr, C. J., and Flores, E. R. (2009) Rescue of key features of the p63-null epithelial phenotype by inactivation of Ink4a and Arf. *EMBO J.* **28,** 1904–1915
44. Schipani, E., and Provot, S. (2003) PTHrP, PTH, and the PTH/PTHrP receptor in endochondral bone development. *Birth Defects Res. C Embryo Today* **69,** 352–362
45. Chen, L., Adar, R., Yang, X., Monsonego, E. O., Li, C., Hauschka, P. V., Yayon, A., and Deng, C. X. (1999) Gly369Cys mutation in mouse FGFR3 causes achondroplasia by affecting both chondrogenesis and osteogenesis. *J. Clin. Invest.* **104,** 1517–1525
46. Pannier, S., Couloigner, V., Messaddeq, N., Elmaleh-Berges, M., Munnich, A., Romand, R., and Legeai-Mallet, L. (2009) Activating Fgfr3 Y367C mutation causes hearing loss and inner ear defect in a mouse model of chondrodysplasia. *Biochim. Biophys. Acta* **1792,** 140–147
47. Kovacs, C. S., Lanske, B., Hunzelman, J. L., Guo, J., Karaplis, A. C., and Kronenberg, H. M. (1996) Parathyroid hormone-related peptide (PTHrP) regulates fetal-placental calcium transport through a receptor distinct from the PTH/PTHrP receptor. *Proc. Natl. Acad. Sci. U. S. A.* **93,** 15233–15238
48. Kuznetsov, S. A., Riminucci, M., Ziran, N., Tsutsui, T. W., Corsi, A., Calvi, L., Kronenberg, H. M., Schipani, E., Robey, P. G., and Bianco, P. (2004) The interplay of osteogenesis and hematopoiesis: expression of a constitutively active PTH/PTHrP receptor in osteogenic cells perturbs the establishment of hematopoiesis in bone and of skeletal stem cells in the bone marrow. *J. Cell Biol.* **167,** 1113–1122
49. Brunner, H. G., Hamel, B. C., and Van, B. H. (2002) The p63 gene in EEC and other syndromes. *J. Med. Genet.* **39,** 377–381

Received for publication September 30, 2009.
Accepted for publication January 14, 2010.